Journal of Medicinal Chemistry

Article

pubs.acs.org/jmc

Order and Disorder: Differential Structural Impacts of Myricetin and Ethyl Caffeate on Human Amylase, an Antidiabetic Target

Leslie K. Williams,[†] Chunmin Li,[†] Stephen G. Withers,*[,‡,†] and Gary D. Brayer[†]

[†]Department of Biochemistry and Molecular Biology, University of British Columbia, Vancouver, British Columbia V6T 1Z3, Canada
[‡]Department of Chemistry, University of British Columbia, Vancouver, British Columbia V6T 1Z1, Canada

ABSTRACT: The increasing prevalence of diabetes has accelerated the search for new drugs derived from natural sources. To define the functional features of two such families of compounds, the flavonols and the ethyl caffeates, we have determined the high-resolution structures of representative inhibitors in complex with human pancreatic α-amylase. Myricetin binds at the active site and interacts directly with the catalytic residues despite its bulky planar nature. Notably, it reduces the normal conformational flexibility of the adjacent substrate binding cleft. In contrast, bound ethyl caffeate acts by disordering precisely those polypeptide chain segments that make up the active site binding cleft. It also operates from binding sites far removed from the active site, a property not observed in any other class of human α-amylase inhibitor studied to date. Given the current inadequacy of drugs directed at diabetes, the use of optimized flavonols and ethyl caffeates may present an alternative therapeutic route.

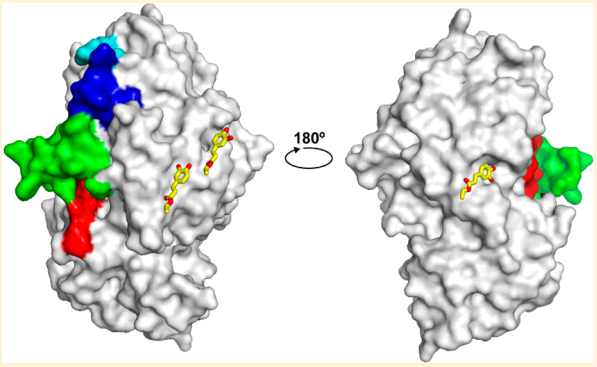

INTRODUCTION

Consumed and subsequently absorbed dietary starches result in a sharp increase in postprandial blood glucose levels. For patients with diabetes, the increased blood glucose levels following a meal present a major challenge in managing hyperglycemia.[3−8] One approach to controlling such undesirable blood glucose spiking events involves the modulation of the activity of the polysaccharide-degrading α-glycosidase enzymes responsible for carbohydrate digestion in the gut by the use of inhibitors ingested along with meals. Three such inhibitors, acarbose, miglitol, and voglibose, have all been used clinically for the treatment of type II diabetes, but these are all found to have disagreeable side effects that interfere with patient compliance.[9−11] These side effects appear to be the consequence of the broad-spectrum inhibition of all intestinal α-glucosidases as well as amylase. This results in small oligosaccharides, which would normally be digested, being allowed to reach the colon where they can be fermented by bacteria, thereby producing bloating, flatulence, and diarrhea. This situation has led to the search for new classes of α-glycosidase inhibitors that demonstrate greater affinity and specificity, with the goal of minimizing currently observed side effect profiles.

Human pancreatic α-amylase (HPA) is a particularly attractive target for the further development of antidiabetic inhibitors that might mitigate postprandial blood glucose levels. Significantly, this enzyme initiates the process of starch digestion, being at the top of the pyramid of subsequent α-glucosidases that eventually degrade the polymeric glucose into the individual glucose molecules that can be absorbed into the bloodstream. Indeed, HPA activity can be directly correlated to blood glucose levels observed after a meal.[3,9]

HPA is an endoglycosidase whose structure and function has been extensively studied.[2,12−15] This enzyme cleaves starch at α-1,4-linked glucose molecules to produce maltose and a range of additional small α-1,4- and α-1,6-linked oligosaccharides that are then further broken down into glucose by α-glucosidases in the gut.[16] The high-resolution structure of HPA shows it to comprise three domains, with the active site located to one end of a triose-phosphate isomerase (TIM) barrel and associated with an extended substrate binding cleft, consistent with its ability to bind polymeric starch molecules.[2] Within this active site cleft are located the three essential carboxylic acid residues (Asp197, Glu233, and Asp300) that catalyze the hydrolysis of glycosidic bonds. Cleavage is accomplished via a classical double displacement mechanism, with net retention of anomeric configuration.[17,18] Detailed kinetic and structural studies have shown that Asp197 acts as the catalytic nucleophile, while Glu233 functions as the acid/base catalyst.[16,19] The side chain of Asp300 is essential in optimizing the orientation of bound substrate in the active site adjacent to the catalytic residues and stabilizing the transition state. Further kinetic and structural characterization of the binding modes of acarbose and related derivatives has been accomplished and has further revealed the nature of the transglycosylation reactions that this enzyme is capable of carrying out.[17,18,20]

Received: September 4, 2012
Published: October 10, 2012

dx.doi.org/10.1021/jm301273u | J. Med. Chem. 2012, 55, 10177−10186

Prominent among alternative classes of inhibitors being studied as prospects having greater specificity and affinity for HPA are derivatives of flavonols[21−30] and caffeic acids[31−33] that occur naturally. Many of these inhibitors have been isolated from herbal remedies that have traditionally been shown to act as antidiabetics. Furthermore, many such derivatives have subsequently been shown to inhibit α-amylases and reduce postprandial hyperglycemia. Studies of flavonols such as myricetin (see Figure 1a) and related derivatives have also

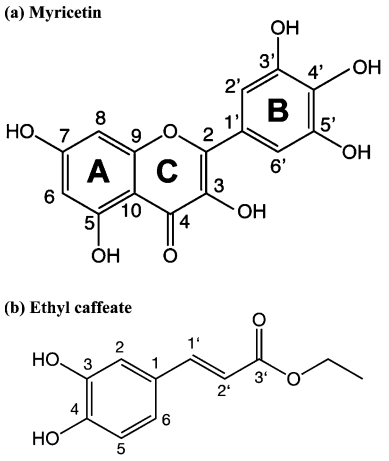

Figure 1. Schematic drawings of the chemical structures of (a) myricetin and (b) ethyl caffeate. Ring designations and atom numbering are also indicated.

been able to relate the potency of these compounds to the number of hydroxyls on the ring structures of the flavonoid scaffold. Similarly, the activities of caffeic acid-based inhibitors have been shown to be dependent on the presence of specific functional groups in the core structure (Figure 1b) and additionally added derivative groups.

At this point an extensive literature concerning the functional traits of flavonoids and caffeic acid derivatives as inhibitors has been published, with research in this area being of considerable interest given the prevalence and upsurge of diabetes in the world population. Nonetheless, significantly impeding progress in the development and optimization of flavonol and ethyl caffeate inhibitors as potential tools in antidiabetic treatments is the lack of high-resolution structural data related to such inhibitory complexes. Structural data of this type are essential to expanding our understanding of the nature of the interactions formed by these compounds in the active site of α-amylases and how such compounds might be utilized more effectively by altering their surface chemistry. To resolve this deficiency and allow for the characterization of the inhibitory modes of action present, we report herein the solution of the individual structures of HPA in complex with myricetin and ethyl caffeate using high-resolution X-ray diffraction methods. The choice of these specific chemical entities is based upon their co-occurrence in a particularly potent amylase inhibitor, montbretin A.[21]

RESULTS

HPA/Myricetin Structure Determination. Excellent high-resolution X-ray diffraction data (1.2 Å, Table 1) were obtained from an HPA crystal soaked in a saturated solution of the inhibitor myricetin (see Figure 1a for the chemical structure). Well-defined electron density in subsequent electron

Table 1. Summary of Structure Determination Statistics

	myricetin/HPA	ethyl caffeate/HPA
Data Collection Parameters		
space group	$P2_12_12_1$	$P2_12_12_1$
unit cell dimension (Å)		
a	52.1	52.1
b	67.4	68.1
c	129.9	125.9
no. of unique reflections	140097	98452
mean $I/\sigma I$[a]	14.7 (5.4)	19.8 (6.8)
multiplicity[a]	4.6 (4.7)	4.8 (4.7)
merging *R* factor[a] (%)	6.4 (28.2)	5.0 (20.1)
max resolution (Å)	1.20	1.35
Structure Refinement Values		
no. of reflections	140013	98366
resolution range (Å)	43.3−1.2	52.1−1.35
completeness[a] (%)	97.8 (98.1)	99.4 (98.2)
no. of protein atoms	3946	3946
no. of inhibitor atoms	23	30
no. of solvent atoms	651	240
av thermal factor (Å^2)		
protein atoms	10.3	19.1
inhibitor atoms	52.1	16.8
solvent atoms	29.9	34.1
overall	13.3	20.1
final *R*-free value[b] (%)	19.8	22.7
final *R* factor (%)	18.0	19.7
Structure Stereochemistry		
rms dev		
bonds (Å)	0.01	0.02
angles (deg)	1.81	2.4

[a]Values in parentheses refer to the highest resolution shell: 1.26−1.20 Å for the myricetin complex and 1.42−1.35 Å for the ethyl caffeate complex. [b]A total of 5% of the data were set aside to calculate *R*-free.

density maps clearly indicated that myricetin had formed a noncovalent complex adjacent to the active site residues of HPA (Figure 2a). Notably, in this bound conformation myricetin makes a total of eight hydrogen bonds in the active site of HPA, four of which are to the two essential catalytic residues Asp197 and Glu233 (Figure 2b). Two of these hydrogen bonds are formed directly to the side chain of Asp197, the residue that acts as the catalytic nucleophile in hydrolysis reactions carried out by HPA on polymeric substrates such as dietary starch.[16,19] Also doubly hydrogen bonded (albeit one through a water molecule) is the side chain of Glu233, which acts as the acid−base catalyst during substrate hydrolysis reactions. Furthermore, myricetin binding strongly influences Asp300, a key residue in the active site that would normally optimize the orientation of a substrate molecule orientation in the S-1 subsite through multiple hydrogen bonds.[18] For this residue, spatial conflicts arise with bound myricetin such that its side chain is displaced away from the active site region through a ∼76° rotation of its χ_1 side chain torsional angle. Overall it would seem that myricetin inhibitory activity has two primary aspects: first in directly engaging the catalytic resides Asp197 and Glu233 through hydrogen bonding and second through steric conflicts that negate the functionality of Asp300.

Additional hydrogen bonds are also formed by myricetin to other residues in the active site that would normally form substrate interactions in the −2 to −3 substrate binding

dx.doi.org/10.1021/jm301273u | J. Med. Chem. 2012, 55, 10177−10186

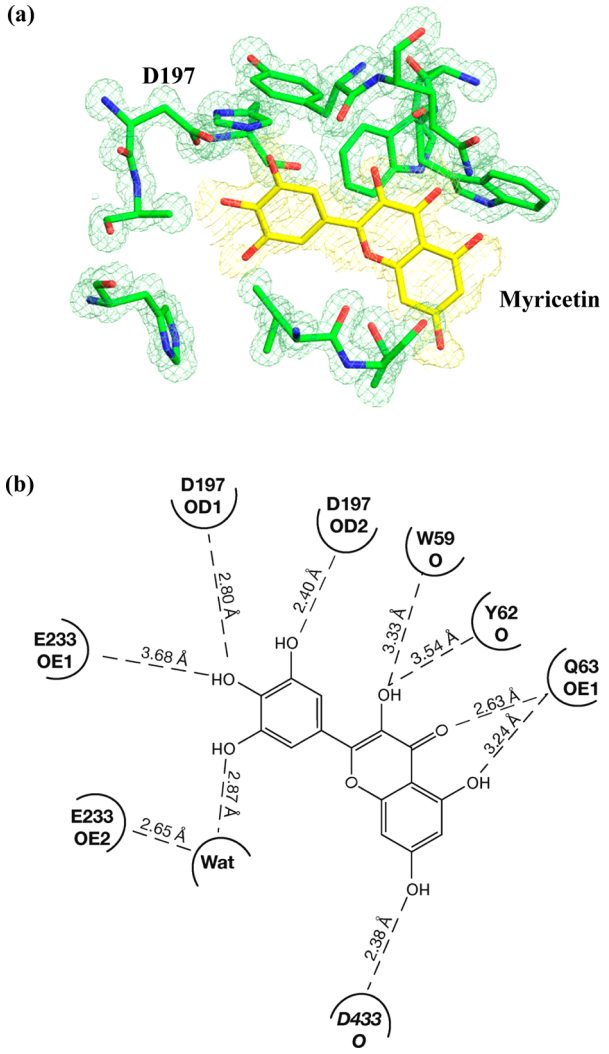

Figure 2. (a) Omit difference electron density map showing the fit of myricetin (yellow backbone, 1.3σ level) and surrounding polypeptide chain (green backbone, 3σ level) in the complex formed by this flavonol in the active site of HPA. (b) Schematic diagram of the hydrogen-bonding interactions formed by myricetin in this complex.

subsites in the elongated substrate binding channel of HPA (Figure 2b).[18,20] Given the highly constrained and nearly planar geometry of myricetin, and therefore its very limited conformational freedom (Figure 1a), it is remarkable that this inhibitor can interact with so many key residues within the active site of HPA at the same time.

Considering the polypeptide chain as a whole, it is evident from Figure 3a that bound myricetin causes minimal perturbation of the overall structure of wild-type HPA (average main chain atom deviation of 0.27 Å). Exceptions to this are two short regions, which are, interestingly, each preceded by a key catalytic residue. One segment that follows the catalytic residue Glu233 involves residues 238 and 239, a region of polypeptide chain that partially forms one side of the active site binding cleft, with particularly close interactions to bound substrates in subsites −1 and −2.[20] Myricetin binding spans this portion of the elongated HPA binding channel, and apparently the dual presence of glycines 238 and 239 provides the necessary polypeptide chain flexibility to allow for the optimization of myricetin interactions. This shifted region is accompanied by a modest drop in thermal factors (Figure 4a), also indicating the influence of myricetin binding on nearby polypeptide chain mobility.

A second segment of polypeptide chain that shifts upon myricetin binding comprises residues 304−306. In uncomplexed HPA, these residues form part of a highly mobile surface loop that is substantially disordered in electron density maps.[2] The primary structural anchor holding this mobile loop close to the enzyme surface is the active site residue Asp300. In earlier studies, we have shown that, upon complexation of substrates or inhibitors in the active site of HPA, the residues of this flexible loop move inward to stabilize ligand binding, resulting in a narrowing of the active site cleft next to the catalytic residues.[16,20] Interestingly, in the case of myricetin, the opposite effect is observed in that this mobile loop is displaced in an outward direction away from the active site cleft. This would appear to be largely a consequence of the displacement by myricetin of the side chain of the key active site residue Asp300, which now projects into the space formerly occupied by His305.

Displacement of the side chain of Asp300 in turn leads to a cascade of nearby polypeptide chain changes that in this case serve to better structure this area such that the nearby polypeptide chain is now readily observable in electron density maps. The most important of these changes involves, first, the displacement of His305, which was initially positioned in the space now occupied by the side chain of Asp300. At its new location the side chain of H305 now forms a hydrogen bond with the side chain of Asp356 (d = 2.8 Å). Second, a new hydrogen bond is formed between the main chain carbonyl of Ala307 and the side chain of Asn301 (d = 3.1 Å). Together these two features appear to promote an overall reorganization of the conformation of the 304−310 loop producing a new pocket into which the reoriented side chain of Asp300 is found. As can be seen in Figure 5a, bound myricetin is in close proximity to this loop as a whole, with residues 304−310 forming one side of that portion of the substrate binding channel that contains this inhibitor. These interactions lead to a significantly lower average main chain thermal B value for this region in the inhibited complex versus that in the wild-type protein (Figure 4a).

HPA/Ethyl Caffeate Structure Determination. It has also proven possible to determine the high-resolution (1.35 Å, Table 1) structure for the complex formed between HPA and the compound ethyl caffeate. The apparent inhibitory mechanism here has a number of unexpected features which clearly delineate it from that observed in the HPA/myricetin complex.

First, electron density maps reveal that a total of three ethyl caffeates are bound in separate pockets on the surface of HPA. In all three cases, ethyl caffeate is found in well-defined electron density, with low average thermal B values (15, 17, and 25 Å^2, respectively), and is present at full occupancy (Figure 6). Despite the apparent tight binding modes, there are no significant perturbations in polypeptide chain conformation in the direct vicinity of any of the ethyl caffeate binding sites.

Second is the unexpected observation that all three ethyl caffeate binding sites are distantly located along the surface of HPA (>20 Å) from the active site and catalytic residues (Figure 5). Indeed, these binding sites are dispersed on the opposite side of HPA from the elongated substrate binding cleft area of this enzyme. One ethyl caffeate forms particularly close interactions with the enzyme surface through a total of five hydrogen bonds (Figure 6). The other two ethyl caffeates bind

dx.doi.org/10.1021/jm301273u | J. Med. Chem. 2012, 55, 10177−10186

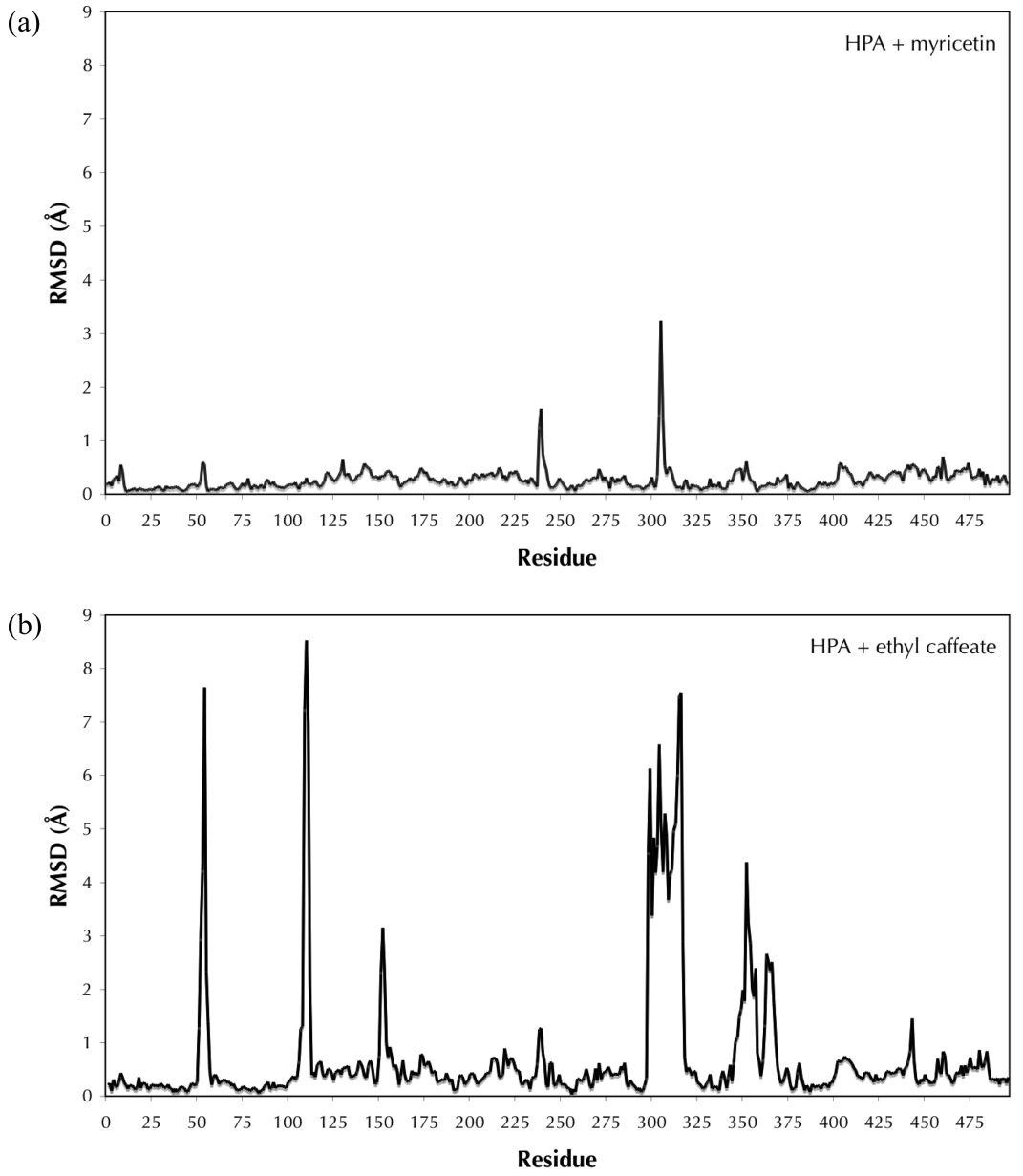

Figure 3. Average root mean squared differences in main chain atomic positions between the (a) myricetin/HPA and (b) ethyl caffeate/HPA complexes and wild-type HPA (PDB ID 1BSI).[15] Notably, myricetin binding in the active site only perturbs a nearby flexible loop adjacent to the catalytic residue Asp300, whereas the three ethyl caffeates bound at remote sites have a much larger impact, causing the positional disordering of four polypeptide chain loops localized in the vicinity of the active site of HPA.

adjacent to one another, although no direct overlapping interactions are apparent between them and they both have unique interactions to the protein surface in their respective binding pockets.

A third unique feature of HPA/ethyl caffeate complexation is that, despite the remote binding sites involved, the triad of inhibitor molecules bound causes a number of segments of polypeptide chain located in the active site region of HPA to become disordered. As a consequence, little or no electron density is observed for residues 51−56, 104−111, 298−315, and 343−358, for a total of 47 residues in all. The significant impact that this disorder has on polypeptide chain placement and average thermal *B* values can be seen in Figures 3b and 4b. Notably, with one exception, these segments of polypeptide chain are well resolved in the free form of the enzyme where each is found to take on a single stable conformation. The exception involves residues 298−315, a segment of polypeptide chain that represents an expansion of a previously observed disordered portion of polypeptide chain in free HPA, comprising residues 304−310.[2,15] These latter residues are normally found to coalesce around substrates and inhibitors bound in the active site region.[17,19,20] Importantly, this also means that the position of the catalytically essential residue D300 is also disordered in this structure. In addition to induced disorder, this latter feature may be a major factor in ethyl caffeate inhibition of HPA.

Significantly, all of the polypeptide chain segments that become disordered in the HPA/ethyl caffeate complex are exclusively located within the elongated substrate binding cleft of HPA. This cleft, and the associated catalytic residues, is positioned to one end of an eight-stranded parallel TIM β-barrel that forms domain A of HPA.[2,15] Notably, in each

dx.doi.org/10.1021/jm301273u | *J. Med. Chem.* 2012, 55, 10177−10186

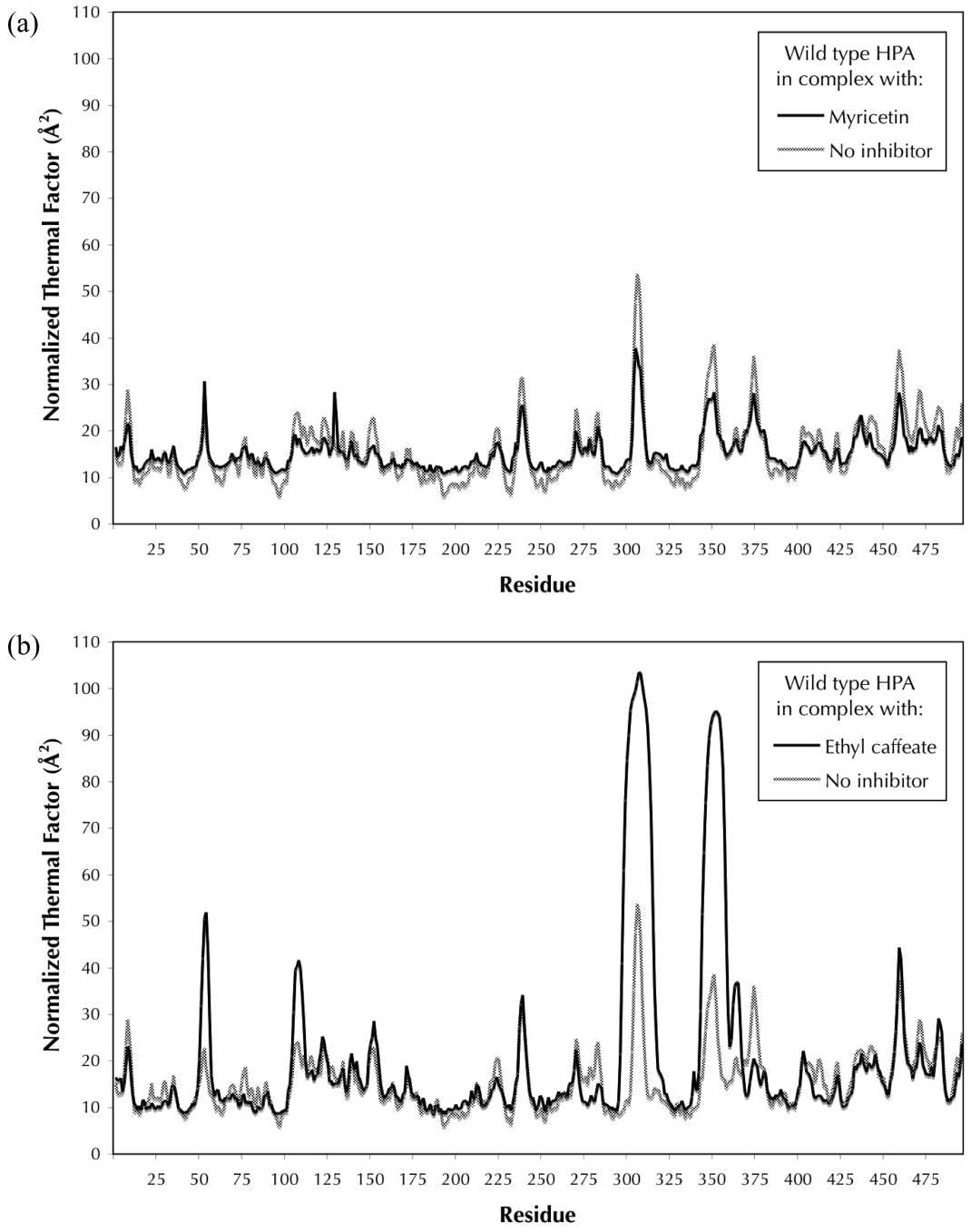

Figure 4. Normalized average main chain thermal *B* factors for the (a) myricetin/HPA and (b) ethyl caffeate/HPA complexes in thick lines. Overlaid are the normalized thermal *B* factors for wild-type HPA as thin lines. While myricetin binding in the active site of HPA leads to more order in a nearby flexible loop next to the active site residue Asp300, in contrast ethyl caffeate binding leads to substantial disorder in four different loops associated with the active site of HPA, centered about residues 53, 107, 306, and 350.

instance, the disordered segments observed upon ethyl caffeate binding constitute what would normally be an ordered coil region of the polypeptide chain following the C-terminal end of a β-strand of the parallel β-barrel and preceding the helical crossover connection to the next strand of the β-barrel. For the disordered segment composed of residues 51−57, this occurs between β-strands 2 and 3 of the β-barrel. For the segments involving residues 104−111, 298−315, and 343−358, the β-strands involved are 3−4, 7−8, and 8−1, respectively. Interestingly, the ethyl caffeate binding sites are all located along the helical wall formed by the crossover connections between β-strands of the β-barrel. Particularly involved are helices 2, 3, and 5. The proximity of these ethyl caffeate sites to the helices that ultimately connect to the observed disordered coil regions is suggestive that this might be the mechanism by which ethyl caffeate remotely exerts its effect on polypeptide chain stability and ultimately enzymatic inhibition.

DISCUSSION

Flavonoid Binding in the HPA Active Site. Naturally occurring flavonoids, such as myricetin, have long been studied for their potential health benefits and, in particular, as potential

dx.doi.org/10.1021/jm301273u | J. Med. Chem. 2012, 55, 10177−10186

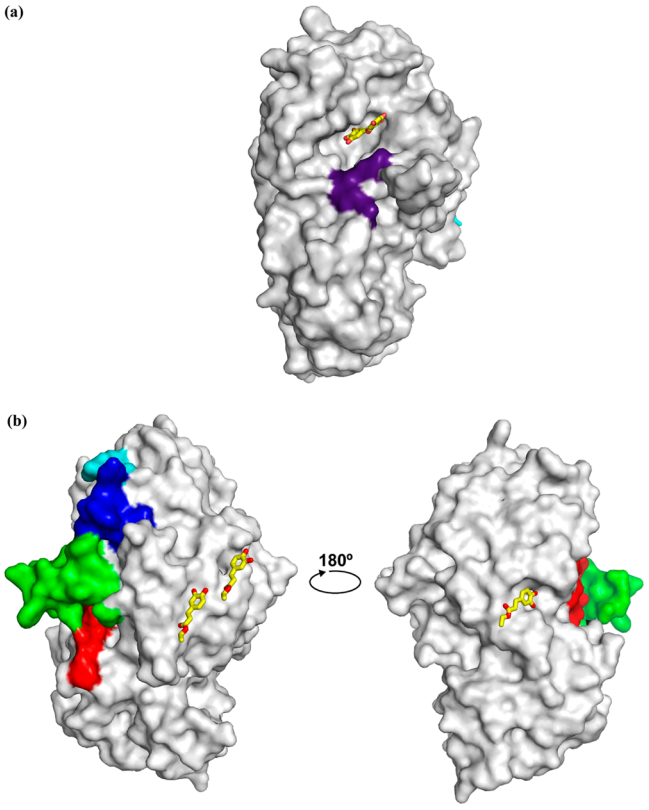

Figure 5. Space-filling representations of the (a) myricetin/HPA and (b) ethyl caffeate/HPA complexes, highlighting the overall positions of bound inhibitors (in yellow). The more ordered loop (residues 305−310) found in the active site of the myricetin/HPA complex is colored purple, while those loops disordered in the active site of the ethyl caffeate/HPA complex are colored magenta (residues 104−111), blue (residues 51−56), green (residues 343−358), and red (residues 298−315). See Figures 3 and 4 for plots of the positional and thermal *B* value differences associated with these changes in polypeptide chain flexibility.

therapeutics for diabetes.[21,22,24,25,27,29,30,34] The primary targets of such inhibitors are the human salivary and pancreatic α-amylases, which are at the top of the starch digestion pyramid that ultimately turns ingested polymeric glucose foodstuffs into monomeric glucose units. This glucose is then, in turn, absorbed into the bloodstream. The potential therapeutic application of flavonoids for diabetic patients would therefore be in first reducing the amount of glucose derived from food and thereby blood glucose levels and second reducing the spiking of glucose concentrations in the bloodstream following a meal. The presence of high blood glucose levels and the glucose spiking phenomenon after meals can in themselves lead to serious medical complications such as progressive worsening of diabetic symptoms and the introduction of comorbidities such as cardiovascular disease, kidney dysfunction, neuropathy, and vision loss.[4−8] Indeed, elevated postprandial glucose levels have been shown to be an accurate predictor of cardiovascular disease associated with diabetes, even more so than conventional markers such as fasting glucose or glycated hemoglobin. Given that the most prevalent form of diabetes is type II and that this form of the disease appears to be closely linked to excessive food consumption, the possibility of developing flavonoid-infused functional foods is being actively investigated as a route to control the onset of diabetes and related obesity issues.[29]

Our current structural analyses illustrate for the first time the mode of binding of a flavonoid in the active site of human pancreatic α-amylase. Importantly, this work provides a solid framework for future studies that would seek to alter myricetin or related flavonoids to create modified inhibitors of higher potency and efficacy. As is readily apparent from Figure 7, myricetin binding is distinct from that determined for other noncovalent and covalent inhibitors such as acarbose, lactams, and elongated 5FIdoF derivatives bound in the extended active site cleft of HPA, which mimic the basic polymeric glucose backbone of normal substrates.[17−20] These types of conventional inhibitors make use of the extended substrate binding cleft of HPA, which contains five high-affinity binding subsites (−3 to +2) for glucose and in which the three active site residues Asp197, Glu233, and Asp300 reside. As our earlier studies have shown, HPA is in fact capable of carrying out both hydrolysis and transglycosylation reactions with bound substrates and inhibitors that mimic such substrates.[17,18]

In contrast, myricetin and related flavonols, with their planar conjugated ring structures, represent inhibitor binding motifs very different from those based on a polymeric glucose framework. Indeed, while myricetin partially fits within the extended substrate binding cleft of HPA, in the area of subsites −3 to −1, it does not form the normal complement of expected interactions in this region. Instead this inhibitor directly engages the catalytic residues Asp197 and Glu233 in an entirely novel manner through hydrogen bonding to the 3′-, 4′-, and 5′-hydroxyls along the planar edge of its B-ring. In this manner, myricetin simultaneously occludes and neutralizes the functionalities of both the catalytic nucleophile and acid/base functions of HPA. Furthermore, the 3′-hydroxyl of the B-ring interacts with the putative nucleophilic water molecule that plays a role in the second half of hydrolysis reactions and is located next to the side chain of Glu233, effectively freezing this functionality in place as well (Figure 3).[16,17,19]

Another unique feature of myricetin binding is the manner in which spatial conflicts lead to a shift in the placement of the side chain of the catalytic residue Asp300 away from the active site (Figure 7). Asp300 displacement results in the widening of the active site cleft due to the coalescence of the nearby substrate binding loop (residues 304−310) into what is now an enzymatically unproductive conformation. Together these structural shifts prevent Asp300 from playing a role in assisting the proper orientation of bound substrates within the active site. Collectively then, myricetin binding interferes with the normal functionality of all three catalytic residues of HPA in a manner not previously observed for other more substrate-like inhibitors.

Comparative Analyses with Flavonoid Modeling Studies. It is also of interest to compare our structural analyses of myricetin binding to HPA, with earlier kinetic (IC_{50}) and "in silico" ligand docking studies involving a series of 19 flavonoids and human salivary amylase.[29] Myricetin was one of the flavonols examined and was found to have an IC_{50} of 30.2 μM and a maximal inhibition of 79%, making it among the top four binders tested. These results can be expected to be roughly comparable to those for HPA, given that this enzyme is highly homologous to that of its salivary isozyme, in terms of both primary sequence and tertiary structure.[2,35] Indeed, the results obtained for myricetin compare favorably with our own more detailed kinetic analysis of myricetin inhibition of HPA, where competitive inhibition with a K_I of 110 μM was found.[21]

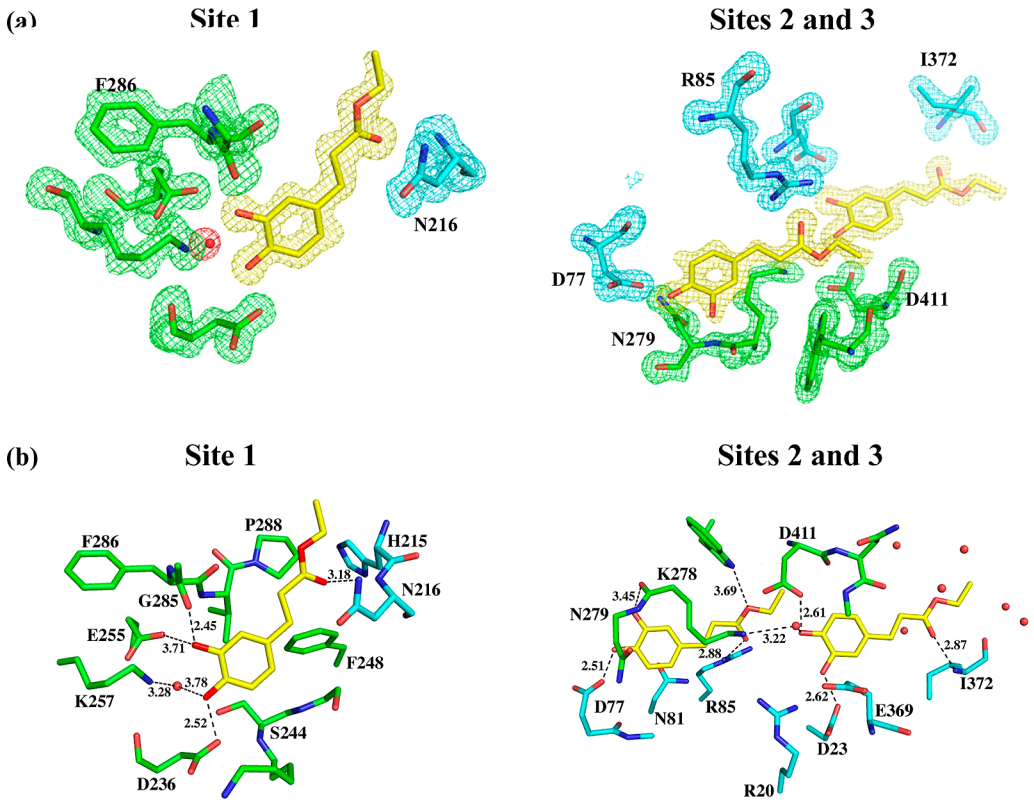

Figure 6. (a) Omit difference electron density maps (2.5σ level) in the vicinity of the three different binding sites for ethyl caffeate on the surface of HPA. Bound ethyl caffeates are shown in yellow, the polypeptide chain of HPA is shown in green, and the polypeptide chain from a symmetry-related HPA is shown in cyan. (b) Detailed structures of these ethyl caffeate binding sites indicating the hydrogen bond interactions formed.

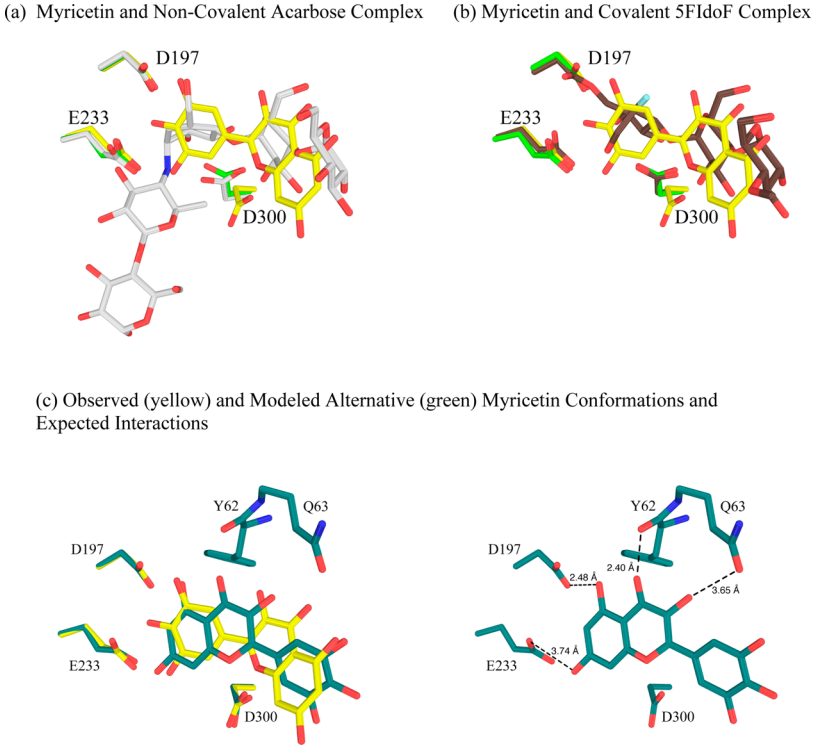

Figure 7. Comparisons of the active site binding modes of myricetin (yellow) and the inhibitor complexes formed by (a) the noncovalent inhibitor acarbose (white)[18,20] and (b) the covalent inhibitor 5FIdoF (brown).[19] In (c) a putative alternative ring placement of myricetin is modeled (dark green) as proposed by computational studies,[29] with the expected hydrogen bonding drawn in schematic fashion. In these drawings the uncomplexed active site polypeptide chain is shown in green.

dx.doi.org/10.1021/jm301273u | J. Med. Chem. 2012, 55, 10177−10186

Although the general aspects of flavonol binding proposed by in silico modeling are in agreement with our structural determination for myricetin binding to HPA, with the B-ring of flavonols placed next to active site residues, there are significant differences in hydrogen-bonding patterns and in planar group stacking interactions. The most notable of these involve catalytic residues. Structural studies show that exceptionally strong hydrogen bonds are formed to each of the OD1 and OD2 carboxylate oxygens of the side chain of Asp197 from the nearby B-ring myricetin 4′- and 5′-hydroxyls, respectively (Figure 2). This is in contrast to the much weaker association suggested from modeling studies wherein these two B-ring hydroxyls form a bifurcated interaction with one of the carboxylate oxygens of Asp197. Similarly, modeling would appear to underestimate the importance of interactions to the catalytic residue Glu233, suggesting a shared hydrogen bond interaction with Asp197 to the 4′-hydroxyl of the B-ring of bound flavonols. Structural studies show a much stronger interaction with this group, incorporating not only a 4′-hydroxyl hydrogen bond, but also a further hydrogen bond to the other carboxylate oxygen of the side chain of Glu233 from the 3′-hydroxyl group of the B-ring through a water molecule. This is the same water molecule that our earlier studies have identified as being positioned to act in the deglycosylation step of the catalytic reaction carried out by HPA.[19,20] These results suggest that flavonol binding to HPA is not only dependent on an optimal spatial fit to the active site region of HPA, but is also highly influenced by the presence of water molecules at the protein/inhibitor contact interface. Undoubtedly, this is especially critical where surface water molecules are active participants in the progress of normal catalytic reactions. The absence of water molecules in modeling studies, coupled with an underestimation of the importance of flavonol interactions with the catalytic residues Asp197 and Glu233, would appear to be responsible for the substantial differences in modeled orientations found for flavonol inhibitors compared to that found for myricetin in structural studies.

Another significant difference between modeling and structural studies would appear to arise from unanticipated positional shifts in surface protein groups in response to myricetin binding. Clearly, such rearrangements can play an important role in inhibitor binding interactions, and many such shifts have been previously observed in the polypeptide chains in the active site cleft of HPA when this enzyme binds substrate-like inhibitors.[17,19,20] While earlier modeling studies attempted to predict these kinds of shifts, clearly this remains a difficult goal given that modeling, with or without consideration for protein surface shifts, resulted in substantially the same predicted bound flavonol inhibitor conformation.[29] Reinforcing the importance of this point is the observed reorientation of the side chain of the catalytic residue Asp300 in structural studies of the myricetin complex. This shift is unique, not being observed in any other HPA/substrate-like inhibitor complex (Figure 7) and, therefore, clearly a significant factor in the unique mode of HPA inhibition by flavonols such as myricetin.

Undoubtedly even more difficult to predict in modeling studies are the secondary effects of shifts in surface protein residues. A case in point is the movement of the side chain of Asp300 in structural studies, which leads to a cascade of related shifts in a nearby loop of polypeptide chain comprised of residues 304−310. This loop is substantially disordered in the wild-type structure of HPA.[2,15] In the structure of the HPA/myricetin complex, not only is this loop restructured, but the side chain of His305 is reoriented and no longer able to form the type of planar stacking interactions that were predicted of this residue in modeling studies. In fact, overall, flavonol $\pi-\pi$ stacking interactions proposed via modeling for side chains such as that of His305 are either absent or substantially different from those found in the experimentally determined structure of the myricetin complex. This would appear to result in large part from unanticipated primary and secondary amino acid shifts in the structure of HPA upon binding to flavonols such as myricetin and the subsequent repositioning of the A−C ring grouping to accommodate them.

Intriguingly, one suggestion that arises from modeling studies is the possibility that flavonols could potentially bind in an alternative conformation in the active site of HPA. In this modeled conformation, the A−C ring component would be positioned adjacent to the catalytic residues Asp197 and Glu233 and the B-ring of the inhibitor would be more remotely positioned in the substrate binding cleft. Assuming our experimentally determined conformation for myricetin binding in the HPA active site, we have explored this possibility by determining a best fit for such a reversed orientation of myricetin. The results of this exercise are illustrated in Figure 7c. While seeming feasible from a strictly spatial fit point of view, such an alternative conformation would likely have considerably less binding affinity due to two factors. First, in this putative complex, the C-ring would present with only two hydroxyl groups immediately adjacent to catalytic residues compared to the three the B-ring was able to provide for hydrogen bonding. Second, the bulky and rigid planar A−C ring grouping would considerably delimit its ability to interact with other groups in this region of the active site binding cleft of HPA.

Ethyl Caffeate-Induced Active Site Disorder. Caffeic acids and their derivatives from natural sources have also been extensively studied for their potential therapeutic properties in relieving symptoms of diabetes.[31−33] Our results show that this small compound represents a class of inhibitor with a completely novel mode of action that involves remote and remarkably precise inducement of polypeptide chain disorder in the active site of HPA (Figures 4 and 5). It would seem that this disordering effect is transmitted via the TIM barrel that makes up the core of the HPA structure and provides the primary platform for catalytic residues and the elongated substrate binding cleft. Significantly, ethyl caffeate only influences the dynamic disorder of the four segments of polypeptide chain (47 residues) that make up the structure of this elongated binding cleft. No other inhibitor class studied to date has this effect on the active site of HPA.

Notably, one aspect that would seem to limit the usefulness of ethyl caffeate as an antidiabetic would be the relatively weak 1.3 mM binding affinity this inhibitor has for HPA.[21] Nonetheless, one could envisage this lack of affinity being enhanced or alternatively compensated for in two ways. First, using our current structural determination of the mode of HPA/ethyl caffeate complexation, it may be possible to increase binding affinity by decorating the core ethyl caffeate compound with other groups to facilitate and strengthen binding to the surface of HPA. Second, it is conceivable from a potential therapeutic point of view that ethyl caffeate could prove to be effective as a companion inhibitor to facilitate the activity of other classes of naturally occurring inhibitors, such as flavonols, that directly target catalytic residues. The dual effect of neutralizing catalytic residues via one class of inhibitor and

inducing disorder in the active site via ethyl caffeate could prove useful in bolstering the effectiveness of both inhibitors.

EXPERIMENTAL SECTION

Materials. All buffer chemicals and reagents were obtained from Sigma/Aldrich Canada unless otherwise specified.

Bacterial Strain, Media, and Plasmids. *Escherichia coli* DH5R subcloning efficiency competent cells were obtained from Gibco BRI and were used for all transformations and DNA manipulations according to standard procedures.[36] *Pichia pastoris* strain GM5011 was used for the expression of wild-type protein. Growth and expression media were prepared as published in the *Pichia* expression kit (Invitrogen). The construction of the expression vectors for wild-type HPA (pPIC9-AMY) has been described elsewhere.[13,15]

HPA Expression and Purification. Transformation of HPA plasmids into *P. pastoris* cells and subsequent selection were carried out according to directions in the *Pichia* expression kit (Invitrogen). Wild-type HPA was deglycosylated and purified using phenyl-Sepharose and Q-Sepharose columns (Pharmacia). The mass and purity of the isolated protein were confirmed using sodium dodecyl sulfate−polyacrylamide gel electrophoresis (SDS−PAGE) and electrospray mass spectrometry. Enzyme concentrations were determined spectrophotometrically using an $A^{0.1\%}$ of 2.2 at 280 nm. Detailed purification protocols for HPA have been described previously.[15−17]

Structure Determinations. Human pancreatic α-amylase was crystallized using the hanging drop vapor diffusion technique at a concentration of 15 mg/mL from 60% 2-methylpentane-2,4-diol and 100 mM cacodylate at pH 7.5. Hanging drops consisted of 5 μL of protein solution mixed with 5 μL of reservoir solution, with high-resolution diffraction-quality crystals growing over a period of one month. Myricetin and ethyl caffeate, both obtained from Alfa Aesar Corp., were dissolved in powder form directly into HPA crystal containing droplets until saturation was reached. Total crystal soaking times of 3 and 15 h were carried out for the myricetin and ethyl caffeate compounds, respectively. Following these soaking procedures, crystals were immediately mounted on diffraction loops and flash frozen in liquid nitrogen in preparation for data collection.

All diffraction data from these two HPA/inhibitor complexes were collected on beamline 11-1 at the Stanford Synchrotron Radiation Lightsource at a wavelength of 0.98 Å using a Mar 325-CCD detector. Diffraction data were processed and reduced using Mosflm and then scaled using Scala.[37] Observed space group and unit cell dimensions (Table 1) indicated that the myricetin/HPA complex containing crystal was isomorphous with that of wild-type HPA, and this latter structure[15] was subsequently used as the starting model for refinement of this complex. In contrast, the ethyl caffeate/HPA complex crystal was found to have a substantially shorter *c*-axial length than crystals of the wild-type protein. In this case, a molecular replacement approach using the CNS software package[38,39] was initially used to obtain a preliminary rotational and translational fit of the structure of wild-type HPA, with this alternative orientation then serving as the starting model for subsequent refinement. All further refinement of the structural models of the myricetin/HPA and ethyl caffeate/HPA complexes was accomplished with CNS,[38,38,39] using alternating cycles of simulated annealing and positional and thermal *B* factor refinements. During this process, the complete polypeptide chains for both inhibitor complexes were examined periodically with F_o-F_c, $2F_o-F_c$, and composite omit electron density maps. Where necessary, manual model rebuilding was performed with COOT.[40]

The preliminary placements of the bound myricetin and ethyl caffeate inhibitors in their respective complexes were readily apparent on the basis of difference electron density maps calculated during the refinement of the protein portion of these complexes. Following inhibitor molecule placements, additional refinement of both the inhibitor and protein portions was carried out to convergence. Inhibitor occupancy was refined to 40% for the myricetin/HPA complex and full occupancy for all three bound molecules in the ethyl caffeate/HPA complex. For both complex structures, solvent peaks were identified in difference electron density maps and their validity monitored on the basis of hydrogen-bonding potential to protein and inhibitor atoms and the refinement of a thermal *B* factor of <65 Å^2. Uniquely, in the case of the HPA/ethyl caffeate complex structure, due to the disorder observed in four segments of polypeptide chain (residues 51−56, 104−111, 298−315, and 343−358), little or no electron density is observed in these areas, and as a consequence, the final refined coordinates for these residues have a high degree of uncertainty. Table 1 provides a summary of data collection, structural refinement, and polypeptide chain geometry statistics for both structure determinations completed.

ASSOCIATED CONTENT

Accession Codes

Coordinates for the two structures described in this work have been deposited in the Protein Data Bank:[1] myricetin/HPA complex, PDB code 4GQR; ethyl caffeate/HPA complex, PDB code 4GQQ.

AUTHOR INFORMATION

Corresponding Author

*Phone: (604) 822-3402. Fax: (604) 822-8869. E-mail: withers@chem.ubc.ca.

Notes

The authors declare no competing financial interest.

ACKNOWLEDGMENTS

This work was supported by an operating grant from the Canadian Institutes of Health Research (CIHR; Reference Number (FRN) 111082). L.K.W. is supported by an Alexander Graham Bell Canada Graduate Scholarship from the Natural Sciences and Engineering Research Council of Canada (NSERC). S.G.W. is supported by a Tier 1 Canada Research Chair. We thank Christopher Overall and Yili Wang for access to equipment and Robert Maurus for technical advice and helpful discussions. Portions of this research were carried out at the Stanford Synchrotron Radiation Lightsource (SSRL), a national user facility operated by Stanford University on behalf of the U.S. Department of Energy, Office of Basic Energy Sciences. The SSRL Structural Molecular Biology Program is supported by the Department of Energy, Office of Biological and Environmental Research, and by the National Institutes of Health, National Center for Research Resources, Biomedical Technology Program, and National Institute of General Medical Sciences. The molecular graphics software package PyMOL was used in drawing the three-dimensional structural figures illustrated herein.[41,42]

ABBREVIATIONS USED

HPA, human pancreatic α-amylase (amino acid numbering is according to a sequence alignment previously published)[2]; 5FIdoF, 5-fluoro-β-L-idosyl fluoride

REFERENCES

(1) Berman, H.; Henrick, K.; Nakamura, H. Announcing the worldwide Protein Data Bank. *Nat. Struct. Biol.* **2003**, *10*, 980.

(2) Brayer, G. D.; Luo, Y.; Withers, S. G. The structure of human pancreatic α-amylase at 1.8 Å resolution and comparisons with related enzymes. *Protein Sci.* **1995**, *4*, 1730−1742.

(3) Mooradian, A. D.; Thurman, J. E. Drug therapy of postprandial hyperglycaemia. *Drugs* **1999**, *57*, 19−29.

(4) Tominaga, M.; Eguchi, H.; Manaka, H.; Igarashi, K.; Kato, T.; Sekikawa, A. Impaired glucose tolerance is a risk factor for cardiovascular disease, but not impaired fasting glucose. The Funagata Diabetes Study. *Diabetes Care* **1999**, *22*, 920−924.

(5) Hanefeld, M.; Fischer, S.; Julius, U.; Schulze, J.; Schwanebeck, U.; Schmechel, H.; Ziegelasch, H. J.; Lindner, J. Risk factors for myocardial infarction and death in newly detected NIDDM: the Diabetes Intervention Study, 11-year follow-up. *Diabetologia* **1996**, *39*, 1577−1583.
(6) Barrett-Connor, E.; Ferrara, A. Isolated postchallenge hyperglycemia and the risk of fatal cardiovascular disease in older women and men. The Rancho Bernardo Study. *Diabetes Care* **1998**, *21*, 1236−1239.
(7) Balkau, B.; Shipley, M.; Jarrett, R. J.; Pyörälä, K.; Pyörälä, M.; Forhan, A.; Eschwège, E. High blood glucose concentration is a risk factor for mortality in middle-aged nondiabetic men. 20-year follow-up in the Whitehall Study, the Paris Prospective Study, and the Helsinki Policemen Study. *Diabetes Care* **1998**, *21*, 360−367.
(8) The DECODE Study Group. Glucose tolerance and mortality: comparison of WHO and American Diabetes Association diagnostic criteria. *Lancet* **1999**, *354*, 617−621.
(9) Krentz, A. J.; Bailey, C. J. Oral antidiabetic agents: current role in type 2 diabetes mellitus. *Drugs* **2005**, *65*, 385−411.
(10) Scott, L. J.; Spencer, C. M. Miglitol: a review of its therapeutic potential in type 2 diabetes mellitus. *Drugs* **2000**, *59*, 521−549.
(11) Chiasson, J. L.; Josse, R. G.; Hunt, J. A.; Palmason, C.; Rodger, N. W.; Ross, S. A.; Ryan, E. A.; Tan, M. H.; Wolever, T. M. The efficacy of acarbose in the treatment of patients with non-insulin-dependent diabetes mellitus. A multicenter controlled clinical trial. *Ann. Intern. Med.* **1994**, *121*, 928−935.
(12) Maurus, R.; Begum, A.; Williams, L. K.; Fredriksen, J. R.; Zhang, R.; Withers, S. G.; Brayer, G. D. Alternative catalytic anions differentially modulate human α-amylase activity and specificity. *Biochemistry* **2008**, *47*, 3332−3344.
(13) Numao, S.; Maurus, R.; Sidhu, G.; Wang, Y.; Overall, C. M.; Brayer, G. D.; Withers, S. G. Probing the role of the chloride ion in the mechanism of human pancreatic α-amylase. *Biochemistry* **2002**, *41*, 215−225.
(14) Maurus, R.; Begum, A.; Kuo, H.; Racaza, A.; Numao, S.; Andersen, C.; Tams, J.; Vind, J.; Overall, C.; Withers, S.; Brayer, G. Structural and mechanistic studies of chloride induced activation of human pancreatic α-amylase. *Protein Sci.* **2005**, *14*, 743−755.
(15) Rydberg, E. H.; Sidhu, G.; Vo, H. C.; Hewitt, J.; Côté, H. C. F.; Wang, Y.; Numao, S.; Macgillivray, R. T. A.; Overall, C. M.; Brayer, G. D.; Withers, S. G. Cloning, mutagenesis, and structural analysis of human pancreatic α-amylase expressed in *Pichia pastoris*. *Protein Sci.* **1999**, *8*, 635−643.
(16) Rydberg, E. H.; Li, C.; Maurus, R.; Overall, C. M.; Brayer, G. D.; Withers, S. G. Mechanistic analyses of catalysis in human pancreatic α-amylase: detailed kinetic and structural studies of mutants of three conserved carboxylic acids. *Biochemistry* **2002**, *41*, 4492−4502.
(17) Numao, S.; Damager, I.; Li, C.; Wrodnigg, T. M.; Begum, A.; Overall, C. M.; Brayer, G. D.; Withers, S. G. In situ extension as an approach for identifying novel α-amylase inhibitors. *J. Biol. Chem.* **2004**, *279*, 48282−48291.
(18) Li, C.; Begum, A.; Numao, S.; Park, K. H.; Withers, S. G.; Brayer, G. D. Acarbose rearrangement mechanism implied by the kinetic and structural analysis of human pancreatic α-amylase in complex with analogues and their elongated counterparts. *Biochemistry* **2005**, *44*, 3347−3357.
(19) Zhang, R.; Li, C.; Williams, L. K.; Rempel, B. P.; Brayer, G. D.; Withers, S. G. Directed "in situ" inhibitor elongation as a strategy to structurally characterize the covalent glycosyl-enzyme intermediate of human pancreatic α-amylase. *Biochemistry* **2009**, *48*, 10752−10764.
(20) Brayer, G. D.; Sidhu, G.; Maurus, R.; Rydberg, E. H.; Braun, C.; Wang, Y.; Nguyen, N. T.; Overall, C. M.; Withers, S. G. Subsite mapping of the human pancreatic α-amylase active site through structural, kinetic, and mutagenesis techniques. *Biochemistry* **2000**, *39*, 4778−4791.
(21) Tarling, C. A.; Woods, K.; Zhang, R.; Brastianos, H. C.; Brayer, G. D.; Andersen, R. J.; Withers, S. G. The search for novel human pancreatic α-amylase inhibitors: high-throughput screening of terrestrial and marine natural product extracts. *ChemBioChem* **2008**, *9*, 433−438.
(22) Liu, I.-M.; Tzeng, T.-F.; Liou, S.-S.; Lan, T.-W. Myricetin, a naturally occurring flavonol, ameliorates insulin resistance induced by a high-fructose diet in rats. *Life Sci.* **2007**, *81*, 1479−1488.
(23) Al-Dabbas, M. M.; Kitahara, K.; Suganuma, T.; Hashimoto, F.; Tadera, K. antioxidant and α-amylase inhibitory compounds from aerial parts of *Varthemia iphionoides* Boiss. *Biosci., Biotechnol., Biochem.* **2006**, *70*, 2178−2184.
(24) Kim, J.; Ryu, Y.; Kang, N.; Lee, B.; Heo, J.; Jeong, I.; Park, K. Glycosidase inhibitory flavonoids from *Sophora flavescens*. *Biol. Pharm. Bull.* **2006**, *29*, 302−305.
(25) Tadera, K.; Minami, Y.; Takamatsu, K.; Matsuoka, T. J. Inhibition of α-glucosidase and α-amylase by flavonoids. *J. Nutr. Sci. Vitaminol.* **2006**, *52*, 149−153.
(26) Gamberucci, A.; Konta, L.; Colucci, A.; Giunti, R.; Magyar, J.; Mandl, J.; Banhegyi, G.; Benedetti, A.; Csala, M. Green tea flavonols inhibit glucosidase II. *Biochem. Pharmacol.* **2006**, *72*, 640−646.
(27) Kim, J.-S.; Kwon, C.-S.; Son, K. H. Inhibition of α-glucosidase and amylase by luteolin, a flavonoid. *Biosci., Biotechnol., Biochem.* **2000**, *64*, 2458−2461.
(28) Funke, I.; Melzig, M. F. Effect of different phenolic compounds on α-amylase activity: screening by microplate-reader based kinetic assay. *Pharmazie* **2005**, *60*, 796−797.
(29) Lo Piparo, E.; Scheib, H.; Frei, N.; Williamson, G.; Grigorov, M.; Chou, C. J. Flavonoids for controlling starch digestion: structural requirements for inhibiting human α-amylase. *J. Med. Chem.* **2008**, *51*, 3555−3561.
(30) Ong, K. C.; Khoo, H. E. Biological effects of myricetin. *Life Sci.* **2000**, *67*, 1695−1705.
(31) Jung, U. J. Antihyperglycemic and antioxidant properties of caffeic acid in db/db mice. *J. Pharmacol. Exp. Ther.* **2006**, *318*, 476−483.
(32) Hsu, F. L.; Chen, Y. C.; Cheng, J. T. Caffeic acid as active principle from the fruit of *Xanthium strumarium* to lower plasma glucose in diabetic rats. *Planta Med.* **2000**, *66*, 228−230.
(33) Yoshida, K.; Hishida, A.; Iida, O.; Hosokawa, K.; Kawabata, J. Flavonol caffeoylglycosides as α-glucosidase inhibitors from *Spiraea cantoniensis* flower. *J. Agric. Food Chem.* **2008**, *56*, 4367−4371.
(34) Li, Y.; Gao, F.; Gao, F.; Shan, F.; Bian, J.; Zhao, C. Study on the interaction between 3 flavonoid compounds and α-amylase by fluorescence spectroscopy and enzymatic kinetics. *J. Food Sci.* **2009**, *74*, C199−C203.
(35) Ramasubbu, N.; Paloth, V.; Luo, Y.; Brayer, G. D.; Levine, M. J. Structure of human salivary α-amylase at 1.6 Å resolution: implications for its role in the oral cavity. *Acta Crystallogr., Sect. D: Biol. Crystallogr.* **1996**, *52*, 435−446.
(36) Sambrook, J.; Fritsch, E.; Maniatis, T. *Molecular Cloning: A Laboratory Manual*; Cold Spring Harbor Laboratory Press: Cold Spring Harbor, NY, 1989.
(37) Collaborative Computational Project. The CCP4 suite: programs for protein crystallography. *Acta Crystallogr., Sect. D: Biol. Crystallogr.* **1994**, *50*, 760−763.
(38) Brünger, A. T.; Adams, P. D.; Clore, G. M.; DeLano, W. L.; Gros, P.; Grosse-Kunstleve, R. W.; Jiang, J. S.; Kuszewski, J.; Nilges, M.; Pannu, N. S.; Read, R. J.; Rice, L. M.; Simonson, T.; Warren, G. L. Crystallography & NMR system: a new software suite for macromolecular structure determination. *Acta Crystallogr., Sect. D: Biol. Crystallogr.* **1998**, *54*, 905−921.
(39) Brunger, A. T. Version 1.2 of the Crystallography and NMR system. *Nat. Protoc.* **2007**, *2*, 2728−2733.
(40) Emsley, P.; Cowtan, K. Coot: model-building tools for molecular graphics. *Acta Crystallogr., Sect. D: Biol. Crystallogr* **2004**, *60*, 2126−2132.
(41) DeLano, W. *The PyMOL Molecular Graphics System*; DeLano Scientific: San Carlos, CA, 2002.
(42) *The PyMOL Molecular Graphics System*, version 1.3r1; Schrödinger, LLC: San Diego, CA, 2010.